Article

J. Biol. Regul. Homeost. Agents. 2024; 38(5): 3849–3860
https://doi.org/10.23812/j.biol.regul.homeost.agents.20243805.304

Effects of TMEM16A Modulation with a High-Calcium Culture Medium on Apoptosis in Enamel Cells of a Fluorosis Tooth Model

Yangyang Yu[1,*,†], Yahui Yan[1,†], Fei Xia[1], Rong Liu[1], Dongrong Zou[1], Haitao Liu[2], Lianfang Wang[3]

[1]Department of Oral Medicine, Huabei Petroleum Administration Bureau General Hospital, 062550 Renqiu, Hebei, China
[2]Huabei Petroleum Administration Bureau General Hospital, 062550 Renqiu, Hebei, China
[3]Department of Pediatrics, Huabei Petroleum Administration Bureau General Hospital, 062550 Renqiu, Hebei, China
*Correspondence: zyy_yyy2023@163.com (Yangyang Yu)
[†]These authors contributed equally.
Published: 1 May 2024

Background: Dental fluorosis is a condition resulting from excessive fluoride intake during tooth development, leading to abnormalities in enamel formation. This study aimed to investigate the impacts of transmembrane protein 16A (TMEM16A) on ameloblast proliferation, apoptosis, and the expression levels of associated genes in a dental fluorosis cell model under high-calcium conditions.

Methods: Ameloblasts were isolated from two C57BL/6 male mice and treated with NaF (3.2 mmol/L) for 24 hours to establish the dental fluorosis cell model. Subsequently, ameloblasts were cultured in Dulbecco's modified eagle medium (DMEM) with varying calcium concentrations such as 2.0, 3.0, or 4.0 mmol/L, along with 10% fetal bovine serum, for 48 h, representing low, medium, and high calcium treatment groups, respectively. Control and NaF model groups were also included. Immunohistochemistry was used to identify the specific marker ameloblastin (AMBN) for ameloblasts. Cell proliferation was assessed using 3-(4,5)-dimethylthiahiazo (-z-y1)-3,5-di-phenytetrazoliumromide (MTT) assay, apoptosis was examined using TUNEL assay, and intracellular Ca^{2+} concentration was measured using fluorescent probes. Moreover, the impacts on the expression of apoptosis-related genes (Bcl2 associated X protein (*Bax*), B-cell lymphoma-2 (*Bcl-2*), nuclear factor kappaB (*NF-κB*), nuclear factor kappa-Bp65 (NF-κBp65)), bone morphogenetic protein-2 (*BMP*-2), and *TMEM16A* were evaluated using quantitative real time polymerase chain reaction (qRT-PCR) and Western blot analysis. Additionally, the effects of the TMEM16A inhibitor T16Ainh-A01 on cell apoptosis and gene expression were investigated.

Results: Compared to the NaF model group, calcium treatment significantly increased AMBN in ameloblasts, promoted cell proliferation ($p < 0.01$), reduced intracellular Ca^{2+} concentration ($p < 0.01$), and inhibited cell apoptosis. Moreover, calcium treatment substantially elevated the expression levels of B-cell lymphoma-2 (Bcl-2) and BMP-2 ($p < 0.05$), while suppressing the expression levels of Bcl2 associated X protein (Bax), nuclear factor kappa-Bp65 (NF-κBp65), and TMEM16A, with the highest efficacy observed in the high-calcium group ($p < 0.05$). Co-treatment with the TMEM16A inhibitor T16Ainh-A01 and high-dose calcium further enhanced cell proliferation ($p < 0.01$), reduced Ca^{2+} concentration ($p < 0.05$), and inhibited cell apoptosis. Additionally, T16Ainh-A01 significantly increased the expression levels of Bcl-2 and BMP-2, while suppressing Bax and NF-κBp65 expression ($p < 0.05$).

Conclusion: Elevated levels of calcium and inhibition of TMEM16A expression can inhibit the apoptosis of ameloblasts caused by fluorosis by regulating the NF-κBp65 signaling pathway and apoptosis-related genes, potentially alleviating fluorosis-induced tooth damage. These findings offer a novel strategy for the prognosis and treatment of dental fluorosis.

Keywords: TMEM16A; dental fluorosis; ameloblasts; cell apoptosis

Introduction

Fluorosis is a dental condition caused by excessive intake of fluoride during tooth development, resulting in abnormal mineralization of enamel. Clinically, this condition manifests through the appearance of white chalky lines or scattered opaque areas on the tooth surface. In severe cases, it may result in the development of enamel defects characterized by pinpoint or banded patterns, affecting either a portion or the entire tooth's surface [1]. Ameloblasts are derived from epithelial cells and play a crucial role in the production of hard tissues, including enamel. Their function includes synthesis and secretion of enamel matrix, as well as its resorption and degradation, and active calcium

Journal of
BIOLOGICAL REGULATORS
and Homeostatic Agents

transport, making them pivotal in enamel formation [2]. Exposure to excessive fluoride, whether acute or chronic, induces changes in the structures of enamel and dentin, inhibiting the formation of ameloblast and odontoblast, impairing matrix synthesis and secretion, and influencing the concentration of Ca^{2+} in the microenvironment of mineralization [3,4]. Despite these observations, the exact mechanisms underlying the pathogenesis of fluorosis have yet to be elucidated.

Apoptosis, a programmed cell death process, plays a crucial role in tooth development. Studies have shown that excessive fluoride intake not only leads to pathological changes such as inflammation and proliferation in ameloblasts but also triggers apoptosis in these cells [5]. Ca^{2+} is involved in regulating various physiological activities of cells and tissues, including metabolism, cell division, and apoptosis [6]. Inadequate dietary calcium intake has been recognized as a significant factor in the development of fluorosis and dental fluorosis [7]. Notably, Ouyang *et al*. [8] observed that increasing calcium intake through dietary sources during tooth development can effectively reduce the severity of dental fluorosis in rats, suggesting the significance of calcium supplementation as a preventive measure against fluorosis to a certain extent. Nonetheless, the precise regulatory mechanisms by which Ca^{2+} influences fluorosis and its potential impact on ameloblast apoptosis remain unclear.

In recent years, there has been considerable research focusing on the molecular mechanism of fluorosis. Particularly, researchers have investigated the role of bone morphogenetic protein (BMP) in the differentiation of ameloblasts and odontoblasts, as well as its involvement in the synthesis and secretion of matrices. The inhibitory impact of fluoride on the expression of BMP-2 in ameloblasts has been documented, consequently affecting enamel matrix secretion and leading to the development of dental fluorosis [9]. Moreover, the nuclear factor kappa-Bp65 (NF-κBp65) pathway plays a crucial role in the development of dental fluorosis [10]. By impacting the expression of BMP-2, NF-κBp65 promotes osteogenic differentiation [11]. Additionally, the dental apoptosis induced by fluorosis includes the involvement of the anti-apoptotic protein B-cell lymphoma-2 (Bcl-2) and the Bcl2 associated X protein (Bax) [12,13]. Understanding the apoptosis process in ameloblasts influenced by fluoride and investigating changes in gene expression are paramount in unraveling the underlying mechanism of dental fluorosis. Transmembrane protein 16A (TMEM16A), also known as Anoctamin-1, represents a calcium-activated chloride ion channel protein that plays a critical role in calcium signaling and intracellular calcium concentration regulation [14,15]. However, the specific role of TMEM16A in the pathogenesis of dental fluorosis remains unclear. Therefore, this study aims to explore the impact of TMEM16A on apoptosis in ameloblasts within a dental fluorosis cell model under high-calcium culture conditions. To achieve this objective, we first established a dental fluorosis cell model by subjecting primary ameloblasts to sodium fluoride (NaF) treatment. Subsequently, we created diverse cell environment by adjusting the Ca^{2+} concentration in the culture medium to simulate various calcium conditions. During this process, we observed the onset of apoptosis and examined the expression of apoptosis-related genes. Additionally, we used the TMEM16A inhibitor T16Ainh-A01 to investigate its influence on apoptosis in ameloblasts within the dental fluorosis cell model.

Methods

Isolation and Culture of Ameloblast Cells

Following the method described by Wang *et al*. [16], two 4-day-old C57BL/6 male mice (Chongqing Enswell Biotechnology Co., Ltd., Chongqing, China) were anesthetized with 0.3% pentobarbital sodium (0.15 mL/10 g) (p3761, Solarbio, Beijing, China). Subsequently, the mice were decapitated, and their mandibular tissues were incised to extract the milk teeth. The extracted teeth were rinsed with phosphate-buffered saline (G0002, Sevier Biotechnology Co., Ltd., Wuhan, China) containing penicillin-streptomycin (C0009, Beyotime Institute of Biotechnology, Shanghai, China). Subsequently, the teeth were incubated with pancreatin (S310KJ, Beyotime Institute of Biotechnology, Shanghai, China) at 37 °C in the presence of 5% CO_2 for 15 minutes. After this, the teeth were rinsed again with PBS containing penicillin-streptomycin. In the next step, the dental tissues were minced into 1 mm^3 pieces and digested with pancreatin for 2 hours at 37 °C in a 5% CO_2 environment. The digestion solution was discarded, and the cells were washed with PBS. Subsequently, the cells were resuspended in Dulbecco's modified eagle medium (DMEM) culture medium (containing 1.2 mmol/L $CaCl_2$ and 1% penicillin-streptomycin, C11995500BT, Gibco, Thermo Fisher Scientific, Inc., Waltham, MA, USA) and then seeded into culture dishes. After 48 hours of incubation at 37 °C in a 5% CO_2 environment, the culture medium was removed, and the non-adherent cells were washed away with PBS. When the primary cultured cells reached 80% to 90% confluence, as observed under an inverted microscope (BLD-200, Cossim, Beijing, China), the old culture medium was discarded. The cells were then washed with PBS (G0002, Wuhan Sevier Biotechnology Co., Ltd., Wuhan, China), and pancreatin was added for digestion. Under microscopic observation, the cells were considered ready for subculture when they became rounded and started to detach from the culture dish. The digestion process was halted by adding a fresh culture medium, and subsequently, the cells were resuspended and sub-cultured in fresh culture dishes at a 1:2 ratio. The sub-cultured cells were further incubated at 37 °C in a 5% CO_2 incubator. Cells were routinely tested for mycoplasma contamination

with a MycoAlert mycoplasma test kit (LT07-701, Lonza, Walkersville, MD, USA) and were found negative for mycoplasma. However, the animal experiments were conducted with the approval of the Ethics Committee of Huabei Petroleum Administration Bureau General Hospital (Ethical Approval No.: 2020-06).

Cell Clustering

Healthy growing cells were selected and resuspended in a culture medium. A mixture of 9 µL of cell suspension and 1 µL of 0.4% Trypan Blue staining solution (R20306, Yuanye Bio-Technology Co., Ltd., Shanghai, China) was prepared for cell counting using a hemocytometer. The cell density was adjusted to 2.0×10^5 cells/mL and subsequently seeded into a 6-well plate. Cells were divided into five groups: the control group, the NaF model group, the low-dose $CaCl_2$ group, the medium-dose $CaCl_2$ group, and the high-dose $CaCl_2$ group. The control group was cultured in DMEM supplemented with 1.2 mmol/L $CaCl_2$. The NaF model group was treated with a culture medium containing 3.2 mmol/L NaF (S111591, Aladdin Biochemical Technology, Shanghai, China) for 24 hours to establish a fluoride dental enamel cell model. The low-dose group was cultured in DMEM containing 2.0 mmol/L $CaCl_2$ and 10% fetal bovine serum (A3161001C, Gibco, Thermo Fisher Scientific, Inc., Waltham, MA, USA) followed by incubation for 48 hours after NaF treatment. Similarly, the medium-dose group was switched to DMEM supplemented with 3.0 mmol/L $CaCl_2$ and 10% fetal bovine serum, while the high-dose group was cultured in DMEM containing 4.0 mmol/L $CaCl_2$ and 10% fetal bovine serum. However, both the medium-dose and high-dose groups were subjected to an additional 48-hour incubation following NaF treatment.

Cells were divided into four groups: the control group, the NaF model group, the high-dose $CaCl_2$ group, and the high-dose $CaCl_2$ + T16Ainh-A01 group. The high-dose $CaCl_2$ + T16Ainh-A01 group was switched to DMEM with 4.0 mmol/L $CaCl_2$ and 10% fetal bovine serum for continued cultivation for 48 h after NaF treatment and then treated with the TMEM16A inhibitor T16Ainh-A01 (10 µmol/L) (552309-42-9, MedChemExpress, Shanghai, China) for an additional 48 hours.

Immunohistochemical Identification of the Enamel-Specific Marker AMBN

After fixing with 4% paraformaldehyde (DF0135, Leagene Biotechnology Co., Ltd., Beijing, China), the cells were treated with goat serum (C0265, Beyotime Institute of Biotechnology, Beijing, China) at room temperature for 60 minutes. Subsequently, the cells were incubated overnight with Anti-AMBN (1:200) (PA5-103108, Thermo Fisher Scientific, Inc., Waltham, MA, USA) at 4 °C. The following day, the cells underwent three PBS washes, and subsequently incubated with Goat Anti-Mouse IgG (H+L) HRP (1:500) secondary antibody (511103, ZEN-BIOSCIENCE, Chengdu, China) at room temperature for 1.5 hours. After three consecutive PBS washes, cells were stained using DAB (ZLI-9019, ZSGB-Bio, Beijing, China) for 1 minute in the dark. Subsequently, they were rinsed with tap water, followed by counterstaining with hematoxylin (G1002, Sevier Biotechnology Co., Ltd., Wuhan, China) for 1 minute. In the next step, the cells were differentiated with 1% hydrochloric acid ethanol (C0163M, Beyotime Institute of Biotechnology, Shanghai, China) for 2 s, and washed with tap water for 10 minutes. Furthermore, the cells were dehydrated with 95% ethanol for 2 minutes, cleared in xylene for 5 minutes, and subsequently mounted with neutral resin (10004160, Pharmaceutical Group Co., Ltd., Harbin, China). Observation under an optical microscope (MF53, Guangzhou MSHOT Optoelectronic Technology, Guangzhou, China) revealed blue cell nuclei and positive regions in brownish-yellow. For quantitative analysis, integrated optical density (IOD) measurements were performed on immunohistochemistry images to calculate the average optical density (AOD) using the following equation: AOD = IOD SUM/area SUM.

MTT Assay

Enamel cells from all five groups (control group, NaF model group, low-dose group, medium-dose group, and high-dose group) were seeded into a 96-well plate, assigning three replicate wells to each group. The culture medium was replaced with a mixture of 90 µL of fresh culture medium and 10 µL of 5 mg/mL 3-(4,5)-dimethylthiahiazo (-z-y1)-3,5-di-phenytetrazoliumromide (MTT) solution (M1020, Solarbio Science & Technology Co., Ltd., Beijing, China) followed by incubation for 4 hours in the presence of CO_2. In the following step, the culture medium was carefully aspirated from each well, and 150 µL of dimethyl sulfoxide (S24295, Yuanye Bio-Technology Co., Ltd., Shanghai, China) was added to dissolve the formazan crystals. The plate was gently shaken on a shaker for 10 minutes to ensure complete dissolution. Finally, the absorbance of each well was measured at 488 nm using a microplate reader (CMax Plus, Molecular Devices Instruments Co., Ltd., San Francisco, CA, USA) and cellular viability was determined using the following formula.

Cell viability (100%) = (Experimental group – Blank group) / (Control group – Blank group) × 100%.

Experimental group: absorbance of cells treated with the MTT solution. Blank group: absorbance of the medium with MTT solution but without cells. Control group: absorbance of untreated cells with the MTT solution.

TUNEL Assay

Initially, the cells were fixed on coverslips, washed with PBS, and subsequently permeabilized using a 0.3% Triton X-100 solution (ST795, Beyotime Institute of Biotechnology, Shanghai, China). Following a 5-minute

Journal of
BIOLOGICAL REGULATORS
and Homeostatic Agents

incubation at room temperature, the cells were stained using a one-step TUNEL apoptosis detection kit (FITC green fluorescence) (G1501, Sevier Biotechnology Co., Ltd., Wuhan, China). Subsequently, the cells were subjected to three consecutive PBS washes, followed by counterstaining with DAPI (C1005, Beyotime Institute of Biotechnology, Shanghai, China) for 5 minutes. The coverslips were then carefully mounted using an anti-fade mounting medium (P0126, Beyotime Institute of Biotechnology, Shanghai, China). Finally, the samples were observed using an optical microscope. The apoptotic positive cell nuclei emitted green fluorescence, while DAPI rendered the nuclei blue fluorescence.

Fluorescent Probe for Detecting Intracellular Ca^{2+} Concentration in Cells

Enamel cells from all five groups (control group, NaF model group, low-dose group, medium-dose group, and high-dose group) were seeded into a 96-well plate, assigning three replicate wells to each group. The used culture medium was removed, and the cells were washed three times with PBS. Subsequently, they were incubated in the dark at 37 °C for 30 minutes with Fluo-3 AM (a Ca^{2+} fluorescent probe) working solution (S1056, Beyotime Institute of Biotechnology, Shanghai, China). After washing three times with PBS, Dulbecco's Phosphate-Buffered Saline (DPBS) (C0221D, Beyotime Institute of Biotechnology, Shanghai, China) was added, and the cells were incubated for 20 minutes. Finally, the detection was performed using a multifunctional microplate reader (SynergyTM 2, Bio-Tek Instruments, Winooski, VT, USA). Using a previously established methodology [17,18], excitation of the Ca^{2+} fluorescence was set at 488 nm, and the emission was measured at 530 nm. The resulting fluorescence values were recorded.

Quantitative Real Time Polymerase Chain Reaction (qPCR)

Total RNA extraction was performed using TRIzol reagent (15596026, Thermo Fisher Scientific, Inc., Waltham, MA, USA) following the manufacturer's instructions. Reverse transcription of RNA to cDNA was conducted using a Goldenstar™ RT6 cDNA Synthesis Kit Ver.2 (TSK302M, Tsingke Biotechnology Co., Ltd., Beijing, China). Moreover, mRNA expression was evaluated using the 2×T5 Fast qPCR Mix (SYBR Green I) reagent kit (TSE002, Tsingke Biotechnology Co., Ltd., Beijing, China). The reaction conditions for RT-qPCR were set as follows: 95 °C for 30 seconds, 95 °C for 5 seconds, and 60 °C for 30 seconds, for a total of 40 cycles. However, glyceraldehyde-3-phosphate dehydrogenase (GAPDH) was used as the internal reference gene, and relative gene expression was assessed using the $2^{-\Delta\Delta Ct}$ method. Specific primers for RT-qPCR are listed in Table 1.

Table 1. A list of primers used in RT-qPCR.

Primers	Sequences
Bax-F	GATCCAAGACCAGGGTGGC
Bax-R	CTTCCAGATGGTGAGCGAGG
Bcl-2-F	GTGGCCTTCTTTGAGTTCGG
Bcl-2-R	CTTCAGAGACAGCCAGGAGAAA
BMP-2-F	GCTGGTCACAGATAAGGCCA
BMP-2-R	TTTCTCGTTTGTGGAGCGGA
NF-κB-F	ACACCTCTGCATATAGCGGC
NF-κB-R	GCAGAGTTGTAGCCTCGTGT
TMEM16A-F	TTGATAACCCTGCCACCGTC
TMEM16A-R	CCTGTGAGGTCCCATCGGTA
GAPDH-F	TGGTGCTGAGTATGTCGTGG
GAPDH-R	GGCGGAGATGATGACCCTTT

Bax, Bcl2 associated X protein; *Bcl-2*, B-cell lymphoma-2; *BMP-2*, bone morphogenetic protein-2; *NF-κB*, nuclear factor kappaB; *TMEM16A*, transmembrane protein 16A; *GAPDH*, glyceraldehyde-3-phosphate dehydrogenase.

Western Blot

Total protein was extracted using RIPA lysis buffer (containing PMSF and a protease inhibitor cocktail) (P0013B, Beyotime, Shanghai, China). Equal amounts of protein from each group were combined with 5× SDS Loading Buffer at a 4:1 ratio and denatured by heating in a metal bath at 100 °C for 6 minutes. After this, 20 µL of each protein sample was subjected to 10% SDS-PAGE electrophoresis for 90 minutes and subsequently transferred onto a PVDF membrane (10600023, Amersham, Freiburg, Germany). The membrane was blocked with 5% skim milk at room temperature for 1 hour, followed by overnight incubation with the primary antibodies (dilution ratio: 1:1000) at 4 °C. The following day, it was incubated with an HRP Goat Anti-Rabbit IgG antibody (dilution ratio: 1:2000) (AS014, ABclonal Technology, Wuhan, China) at room temperature for 1 hour. Protein bands were visualized using an ECL exposure solution (34580, Thermo Fisher Scientific, Inc., Waltham, MA, USA) and analyzed with a nucleic acid and protein gel imaging system (Universal Hood II, Bio-Rad, San Diego, CA, USA). Band intensities were assessed using ImageJ (version 1.48b, National Institutes of Health, Bethesda, MD, USA). The primary antibodies Bax (A19684), Bcl-2 (A0208), BMP-2 (A14708), nuclear factor kappa-B p65 (NF-κBp65) (A2547), TMEM16A (A10498), and GAPDH (AS014) were purchased from ABclonal Technology (Wuhan, China).

Statistical Analysis

Data analysis was performed using GraphPad Prism version 8 (GraphPad Software Company, San Diego, CA, USA). One-way analysis of variance (ANOVA) followed by Tukey's post hoc test was employed for multiple group

comparison. The data were presented as mean ± standard deviation. Each experiment was conducted in triplicate. Statistical significance was determined at a p value < 0.05.

Results

Different Calcium Concentration Culture Medium Treatments and Their Impact on the Proliferation, Apoptosis, and Ca^{2+} Concentration of Fluorosed Enamel Cells

To elucidate the effects of different calcium concentrations on the proliferation and apoptosis of ameloblasts in fluorosed enamel, ameloblast cell models were cultured on DMEM culture media containing 2.0 mmol/L, 3.0 mmol/L, and 4.0 mmol/L $CaCl_2$, respectively. Immunohistochemical staining revealed positive AMBN staining in brownish-yellow. As depicted in Fig. 1A, except for the NaF group, ameloblasts in all other groups exhibited brownish-yellow staining, indicative of AMBN expression. As the concentration of Ca^{2+} increased, ameloblasts proliferation was observed (Fig. 1A). MTT assay results indicated a significant decrease in ameloblast cell viability within all groups following NaF treatment compared to the control group ($p = 6.87 \times 10^{-11}$). However, compared to the NaF model group, all three concentrations of Ca treatment significantly promoted cell proliferation ($p = 0.01$, $p = 2.00 \times 10^{-6}$, $p = 1.27 \times 10^{-8}$), with the high calcium group (4.0 mmol/L) exerting the most notable effect on cell proliferation (Fig. 1B). As Ca^{2+} acts as a major intracellular messenger, abnormal elevations in its concentrations can trigger apoptosis. Immunofluorescence analysis revealed a significant increase in the Ca^{2+} concentration in ameloblasts following NaF treatment compared to the control group ($p = 6.14 \times 10^{-10}$). Conversely, treatment with the three different concentrations of Ca^{2+} led to a significant decrease in the Ca^{2+} concentration in ameloblasts ($p = 0.005$, $p = 1.00 \times 10^{-6}$, $p = 3.85 \times 10^{-9}$), with the high calcium group (4.0 mmol/L) exhibiting the lowest Ca^{2+} concentration (Fig. 1C). Furthermore, TUNEL analysis revealed that NaF treatment increased the apoptosis rate compared to the control group. While all three concentrations of $CaCl_2$ treatment significantly inhibited cell apoptosis, with the high calcium group (4.0 mmol/L) showing the most substantial inhibitory effect on cell apoptosis (Fig. 1D).

Impacts of Treatment with Culture Media Containing Varying Calcium Concentrations on the Expression of Apoptosis-Related Proteins in Fluorosed Enamel Ameloblasts

The qPCR and WB analysis indicated that, as compared to the control group, NaF treatment resulted in a substantial increase in the expression of Bax, *NF-κB*, NF-κBp65, and TMEM16A within enamel-forming cells of all groups (mRNA expression: $p = 1.97 \times 10^{-12}$, $p = 1.13 \times 10^{-10}$, $p = 1.53 \times 10^{-10}$; protein expression: $p = 4.27 \times 10^{-8}$, $p = 5.32 \times 10^{-10}$, $p = 2.43 \times 10^{-8}$). Conversely, the expression levels of Bcl-2 and BMP-2 were significantly reduced upon NaF treatment (mRNA expression: $p = 4.70 \times 10^{-12}$, $p = 2.14 \times 10^{-12}$; protein expression: $p = 2.61 \times 10^{-9}$, $p = 3.29 \times 10^{-8}$). Moreover, compared to the NaF model group, calcium treatment significantly decreased the expression of Bax, *NF-κB*, NF-κBp65, and TMEM16A, in a concentration-dependent manner (mRNA expression: $p = 3.26 \times 10^{-12}$, $p = 3.20 \times 10^{-10}$, $p = 3.15 \times 10^{-9}$; protein expression: $p = 2.00 \times 10^{-6}$, $p = 3.99 \times 10^{-8}$, $p = 4.22 \times 10^{-7}$). Conversely, the expression of Bcl-2 and BMP-2 in enamel-forming cells significantly elevated after calcium treatment, with the highest expression level observed in the H-Ca^{2+} group (4.0 mmol/L) (mRNA expression: $p = 8.84 \times 10^{-10}$, $p = 9.67 \times 10^{-12}$; protein expression: $p = 2.07 \times 10^{-7}$, $p = 2.00 \times 10^{-6}$) (Fig. 2).

Effects of TMEM16A Inhibitor under High-Calcium Medium on Proliferation, Apoptosis, and Ca^{2+} Concentration of Fluorosis Teeth Enamel Cells

To investigate the role of TMEM16A in the proliferation and apoptosis of ameloblasts under high-calcium culture conditions, ameloblasts were treated with 4.0 mmol/L $CaCl_2$ along with the TMEM16A inhibitor T16Ainh-A01. MTT results revealed a significant decrease in cell viability in all groups following NaF treatment compared to the control group ($p = 5.85 \times 10^{-8}$). However, in comparison to the NaF model group, both the H-Ca^{2+} and H-Ca^{2+}+T16Ainh-A01 groups significantly promoted ameloblast proliferation. Interestingly, the H-Ca^{2+}+T16Ainh-A01 group showed significantly decreased cell proliferation compared to the H-Ca^{2+} group ($p =$ 003, Fig. 3A). Fluorescent probe analysis revealed that NaF treatment elevated intracellular Ca^{2+} concentration in ameloblasts across all groups. However, high-calcium treatment resulted in a significant reduction in the Ca^{2+} concentration compared to the NaF model group ($p = 4.00 \times 10^{-5}$). However, the H-Ca^{2+}+T16Ainh-A01 group exhibited a significantly lower calcium concentration than the H-Ca^{2+} group ($p = 0.03$, Fig. 3B). Furthermore, TUNEL assay results showed that NaF treatment enhanced the apoptosis rate in ameloblasts in all groups compared to the control group. However, high-calcium treatment significantly suppressed apoptosis, and the H-Ca^{2+}+T16Ainh-A01 group showed fewer apoptotic cells than the H-Ca^{2+} group (Fig. 3C).

Impact of TMEM16A Inhibitor on the Expression of Apoptosis-Related Proteins in Ameloblasts of Fluorosis Enamel under High-Calcium Culture Conditions

The qPCR and WB analysis indicated significantly reduced expression levels of Bax, *NF-κB*, NF-κBp65, and TMEM16A in the control group (mRNA expression: $p = 2.11 \times 10^{-7}$, $p = 3.71 \times 10^{-10}$, $p = 2.38 \times 10^{-7}$; pro-

Journal of
BIOLOGICAL REGULATORS
and Homeostatic Agents

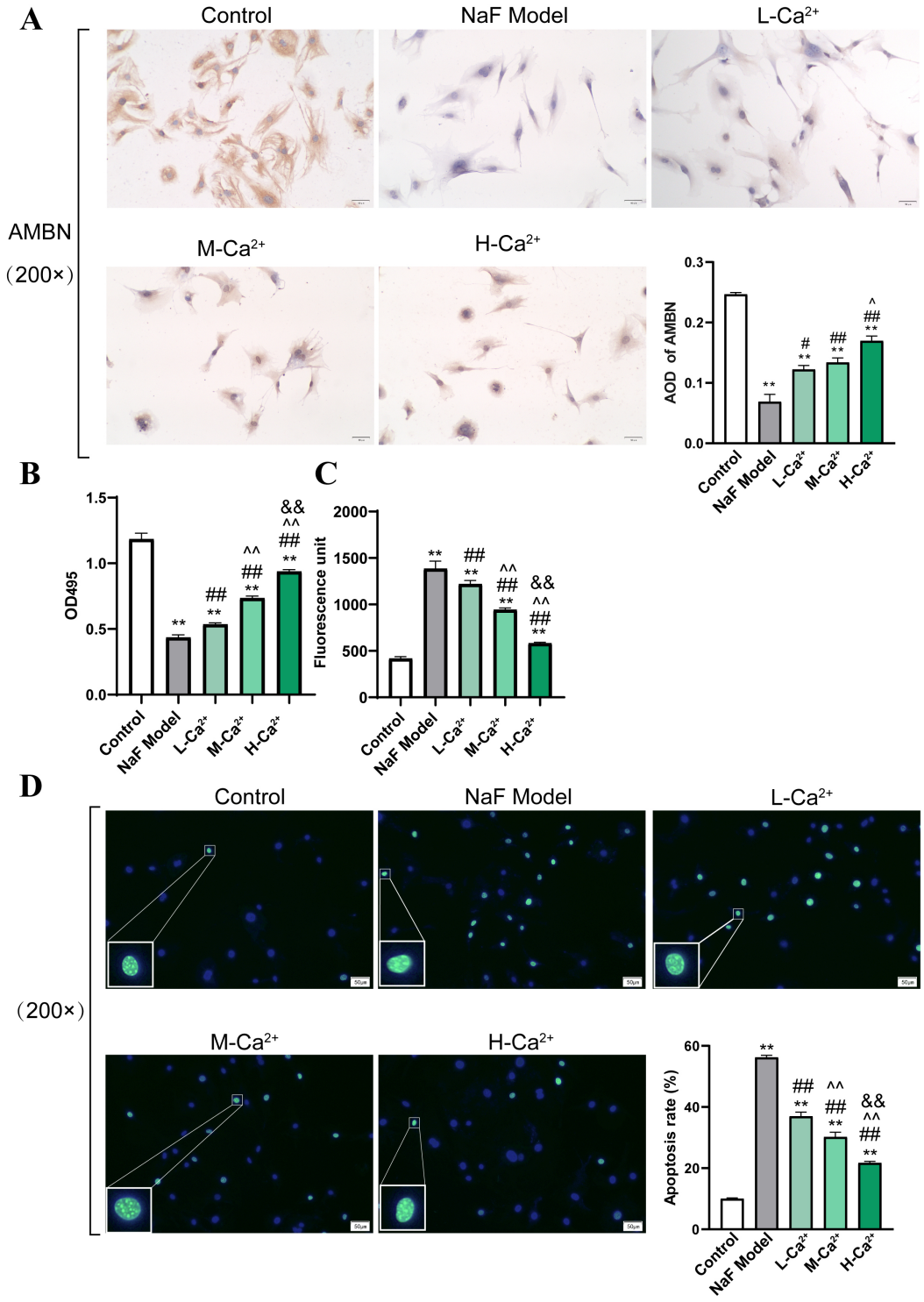

Fig. 1. Impacts of calcium treatment on the proliferation and apoptosis of ameloblasts in a fluorosed enamel cell model. (A) Immunohistochemical identification of the ameloblast-specific marker Ameloblastin (AMBN). Scale bar: 50 μm. (B) 3-(4,5)-dimethylthiahiazo (-z-y1)-3,5-di-phenytetrazoliumromide (MTT) assay for cell proliferation. (C) Fluorescent probe assessment of intracellular Ca^{2+} concentration. (D) TdT-mediated dUTP Nick-End Labeling (TUNEL) assay for cell apoptosis. Scale bar: 50 μm. A one-way Analysis of Variance (ANOVA) followed by a post hoc test using Tukey's test was used for multiple group comparisons. $^{**}p < 0.01$ in comparison to the control group. $^{\#}p < 0.05$ and $^{\#\#}p < 0.01$ in comparison to the NaF model group. $^{\wedge}p < 0.05$ and $^{\wedge\wedge}p < 0.01$ in comparison to the L-Ca^{2+} group. $^{\&\&}p < 0.01$ in comparison to the M-Ca^{2+} group. n = 3.

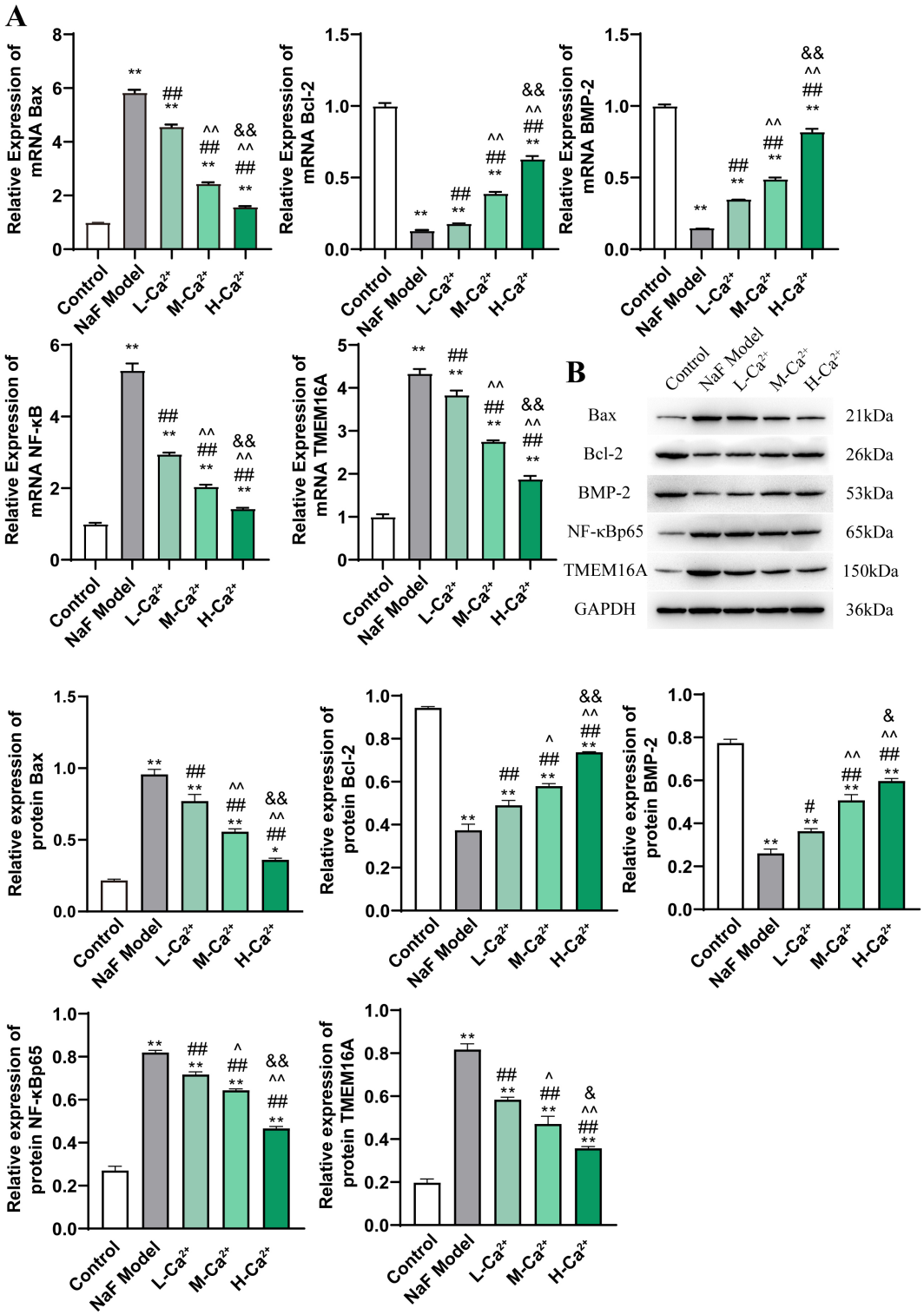

Fig. 2. Impacts of calcium treatment on the expression of Bcl2 associated X protein (Bax), B-cell lymphoma-2 (Bcl-2), bone morphogenetic protein-2 (BMP-2), nuclear factor kappaBp65 (NF-κBp65), and transmembrane protein 16A (TMEM16A) in enamel-forming cells of the fluorosis tooth cell model. (A) Quantitative real time polymerase chain reaction (qPCR) for the assessment of mRNA expression in enamel cells for *Bax*, *Bcl-2*, *BMP-2*, nuclear factor kappaB (*NF-κB*), and *TMEM16A*. (B) Western blot analysis to evaluate the protein expression of Bax, Bcl-2, BMP-2, NF-κBp65, and TMEM16A. A one-way ANOVA followed by a post hoc test using Tukey's test was used for multiple group comparisons. $^{*}p < 0.05$ and $^{**}p < 0.01$ in comparison to the control group. $^{\#}p < 0.05$ and $^{\#\#}p < 0.01$ in comparison to the NaF model group. $^{\wedge}p < 0.05$ and $^{\wedge\wedge}p < 0.01$ in comparison to the L-Ca^{2+} group. $^{\&}p < 0.05$ and $^{\&\&}p < 0.01$ in comparison to the M-Ca^{2+} group. n = 3.

Journal of
BIOLOGICAL REGULATORS
and Homeostatic Agents

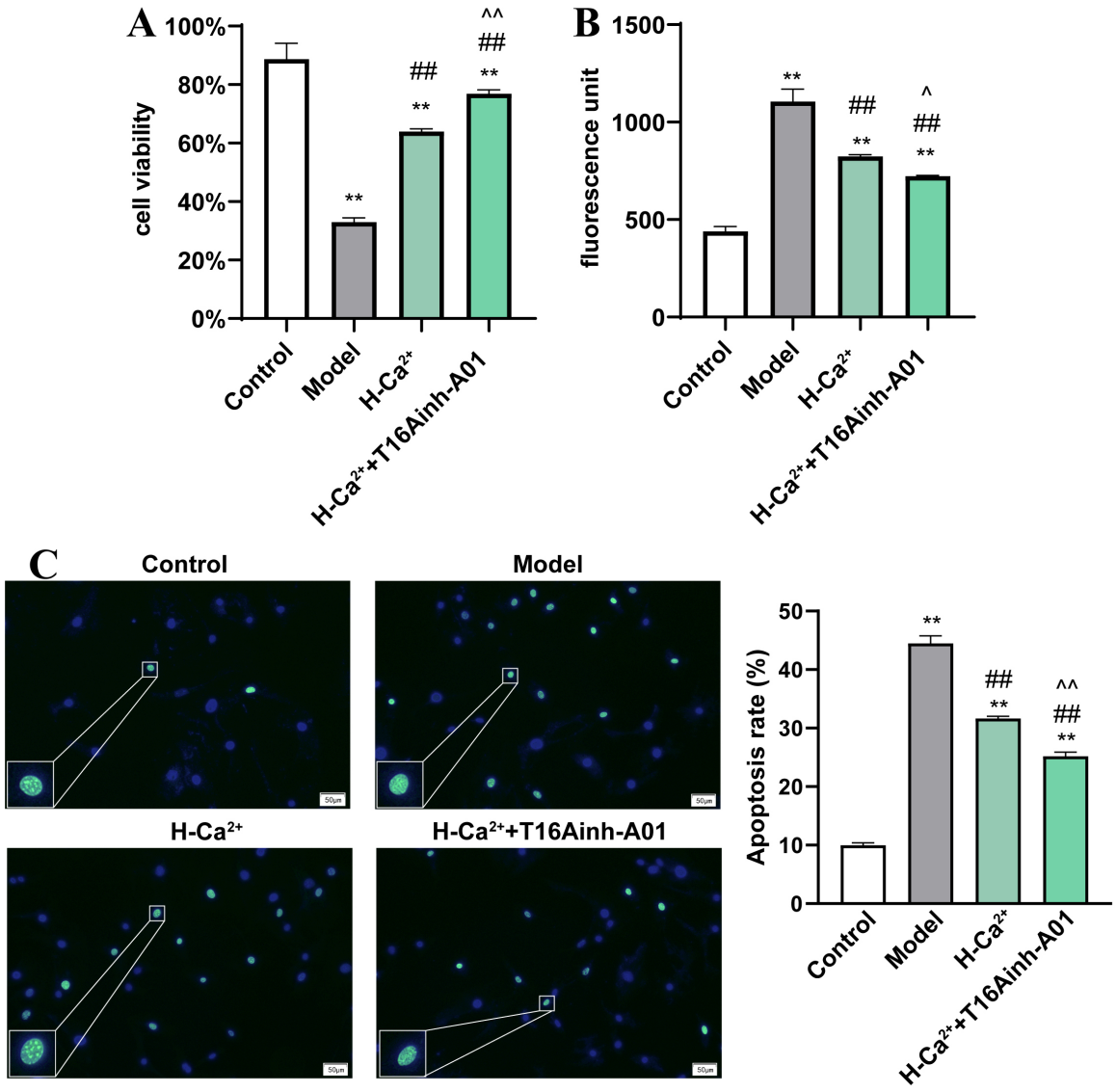

Fig. 3. Impact of T16Ainh-A01 on the proliferation and apoptosis of fluorosis enamel cell model ameloblasts under high-calcium culture conditions. (A) Cell proliferation detection by using MTT. (B) Intracellular Ca^{2+} concentration measurement with a fluorescent probe. (C) Cell apoptosis assessment using TUNEL assay. A one-way ANOVA followed by a post hoc test using Tukey's test was used for multiple group comparisons. Scale bar: 50 μm. $^{**}p < 0.01$ in comparison to the control group. $^{\#\#}p < 0.01$ in comparison to the NaF model group. $^{\wedge}p < 0.05$, $^{\wedge\wedge}p < 0.01$ in comparison to the H-Ca^{2+} group. n = 3.

tein expression: $p = 1.00 \times 10^{-6}$, $p = 1.21 \times 10^{-7}$, $p = 1.00 \times 10^{-6}$). Conversely, the expression levels of Bcl-2 and BMP-2 were the highest in the control group (mRNA expression: $p = 6.52 \times 10^{-8}$, $p = 4.29 \times 10^{-9}$; protein expression: $p = 6.00 \times 10^{-6}$, $p = 4.15 \times 10^{-7}$). Moreover, compared to the NaF model group, high-calcium treatment reduced the expression of Bax, *NF-κB*, NF-κBp65, and TMEM16A in enamel-forming cells (mRNA expression: $p = 1.74 \times 10^{-4}$, $p = 2.57 \times 10^{-9}$, $p = 9.70 \times 10^{-5}$; protein expression: $p = 0.01$, $p = 9.70 \times 10^{-5}$, $p = 0.004$). However, the H-Ca^{2+}+T16Ainh-A01 group exhibited the lowest levels (mRNA expression: $p = 1.18 \times 10^{-4}$, $p = 0.01$, $p = 2.36 \times 10^{-4}$; protein expression: $p = 0.006$, $p = 0.001$, $p = 0.008$). Furthermore, compared to the NaF model group, high-calcium treatment significantly increased the expression of Bcl-2 and BMP-2 in enamel-forming cells (mRNA expression: $p = 0.001$, $p = 7.06 \times 10^{-7}$; protein expression: $p = 0.006$, $p = 0.001$). However, their levels were higher in the H-Ca^{2+}+T16Ainh-A01 group compared to the H-Ca^{2+} group (mRNA expression: $p = 7.90 \times 10^{-5}$, $p = 0.002$; protein expression: $p = 0.02$, $p = 1.36 \times 10^{-4}$, Fig. 4).

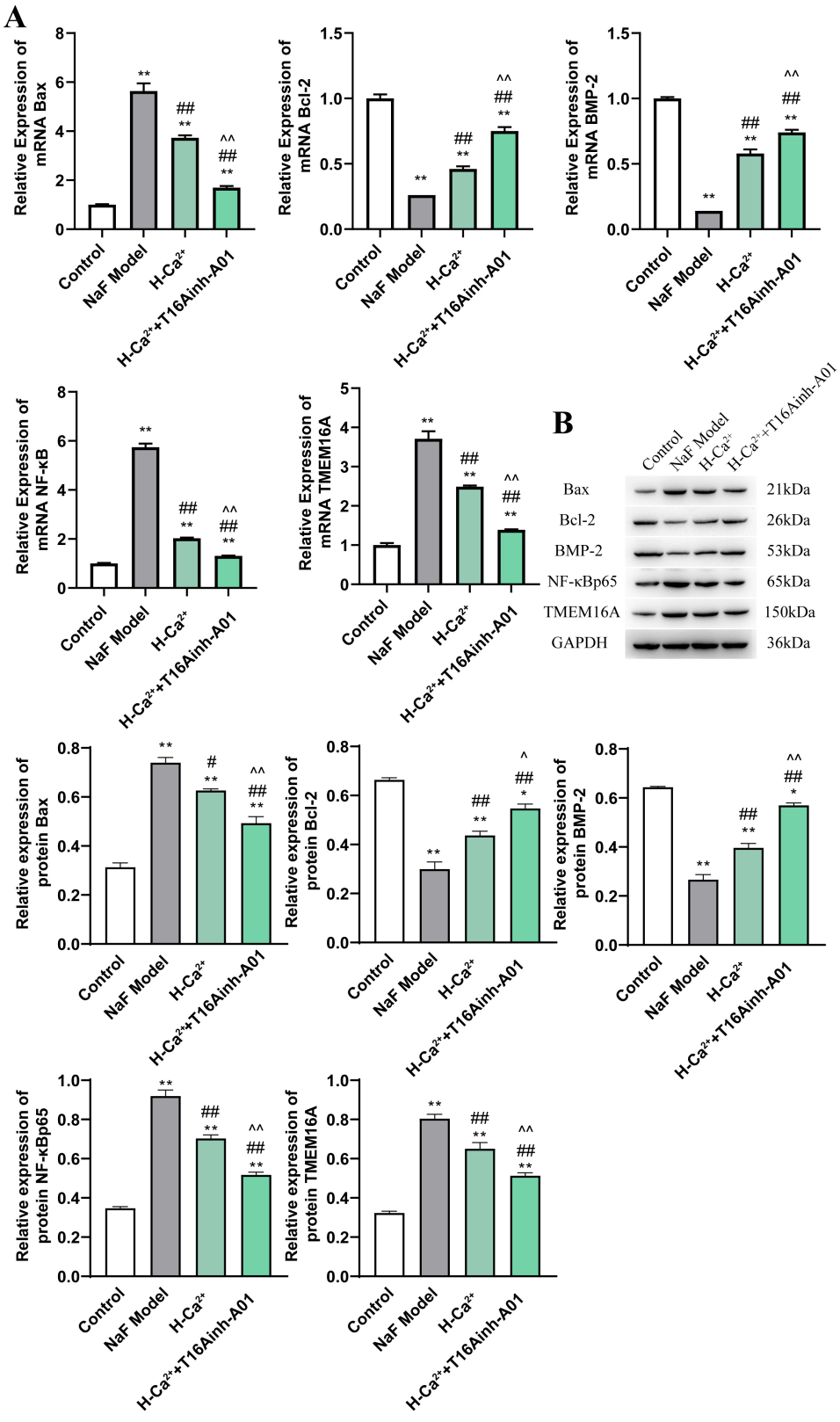

Fig. 4. Impact of T16Ainh-A01 on the expression of Bax, Bcl-2, BMP-2, NF-κBp65, and TMEM16A in enamel-forming cells under high-calcium culture conditions. (A) qPCR analysis of mRNA expression of *Bax*, *Bcl-2*, *BMP-2*, *NF-κB*, and *TMEM16A* in enamel-forming cells. (B) WB analysis of protein expression of Bax, Bcl-2, BMP-2, NF-κBp65, and TMEM16A in enamel-forming cells. Glyceraldehyde-3-phosphate dehydrogenase (*GAPDH*) was used as the internal reference gene. A one-way ANOVA followed by a post hoc test using Tukey's test was used for multiple group comparisons. $^{*}p < 0.05$, $^{**}p < 0.01$ in comparison to the control group. $^{\#}p < 0.05$, $^{\#\#}p < 0.01$ in comparison to the NaF model group. $^{\wedge}p < 0.05$, $^{\wedge\wedge}p < 0.01$ in comparison to the H-Ca^{2+} group. n = 3.

Journal of
BIOLOGICAL REGULATORS
and Homeostatic Agents

Discussion

Fluoride, an essential trace element recognized for its anti-cavity properties, may lead to a specific enamel development disorder called dental fluorosis when consumed excessively during teeth mineralization. Studies have shown that dietary calcium intake can protect against the toxic impacts of fluoride by reducing its absorption [19,20]. Yu *et al*. [21] observed a gradual increase in both blood and bone fluoride levels in rats after excessive fluoride intake, particularly in those subjected to low-calcium and normal-calcium treatment, while high-calcium-treated rats showed minimal changes. Furthermore, dental fluorosis was most severe in the low-calcium group and less severe in the high-calcium group, suggesting that high calcium counteracts the toxic effects of fluoride on teeth by reducing fluoride accumulation in the body. Calcium supplementation leads to the formation of insoluble calcium fluoride within the intestine, which is subsequently excreted from the body through the processes of digestion and metabolism. Additionally, excess calcium may bind with fluoride in the local environment, thereby reducing free fluoride [22]. Previous research has demonstrated the impact of high fluoride concentrations on apoptosis in primary rat ameloblast cells [16]. In this study, we established a dental fluorosis cell model by using C57BL/6 mice ameloblast cells. The cells were treated with NaF to investigate the influence of different calcium concentrations in the culture medium on apoptosis of ameloblast cells. Initially, we identified ameloblast cells through AMBN immunohistochemistry to ensure the specificity of our cell model. MTT assay results indicated that calcium treatment significantly promoted ameloblast cell proliferation, with the most favorable outcomes observed in the high calcium group. This finding suggests that high calcium mitigates fluoride toxicity to some extent, consistent with the observations made by Yu *et al*. [21]. Ca^{2+} plays a crucial role as an intracellular messenger in maintaining normal cell structure and function [23]. Sodium fluoride (100 ng/mL) has been shown to activate cell membrane Ca^{2+} channels, causing a rapid increase in intracellular Ca^{2+} concentration in osteoblasts [24]. Disruption of calcium balance due to various harmful factors can disturb Ca^{2+} distribution, resulting in abnormally high intracellular Ca^{2+} levels, ultimately triggering cell apoptosis [25]. In this study, we observed that NaF (3.2 mmol/L) significantly increased intracellular Ca^{2+} concentration in ameloblast cells, thereby promoting cell apoptosis, which aligns with the findings reported by Zhang *et al*. [26]. Conversely, calcium significantly reduced intracellular Ca^{2+} concentration in ameloblast cells, inhibiting cell apoptosis. However, the high-calcium group exhibited the most pronounced effect, suggesting that this may be one of the mechanisms underlying its anti-apoptotic action.

Apoptosis is a crucial cellular process for maintaining the homeostasis of normal tissues. Previous research has demonstrated the significant role of the Bcl-2 family members in the process of apoptosis, which can be classified into anti-apoptotic proteins and pro-apoptotic proteins based on their structural and functional characteristics [27]. The anti-apoptotic protein Bcl-2 can inhibit the activation of apoptosis-related genes by suppressing DNA transcription. When the pro-apoptotic protein Bax is highly expressed, it forms a heterodimer with Bcl-2, leading to the inactivation of Bcl-2 and enhancing cell apoptosis [28]. Furthermore, NaF has been shown to downregulate the expression of Bcl-2 mRNA in osteoblasts while upregulating the expression of Bax mRNA, thereby initiating the mitochondrial apoptosis signaling pathway [29]. Zhao *et al*. [30] proposed that the toxic effect of fluoride on ameloblasts could induce cell apoptosis by inhibiting Bcl-2 expression, thus affecting the development of enamel and ultimately leading to abnormal tooth development. Furthermore, during tooth embryonic development, BMPs serve as signaling molecules between the epithelium and mesenchyme. BMPs play crucial roles in the differentiation, matrix synthesis, and secretion of odontoblasts and ameloblasts. Among them, BMP-2 maintains continuous expression during the differentiation process of odontoblasts and ameloblasts [31,32]. It has been suggested that under the influence of excessive fluoride, the expression of BMP-2 protein is inhibited, which hinders the differentiation of ameloblasts and subsequent matrix secretion, thereby contributing to the formation of dental fluorosis [33]. Nuclear factor κB (NF-κBp65) is an important nuclear transcription factor within cells, and chronic fluoride poisoning has been shown to affect the transcriptional regulation of NF-κBp65 [34]. Research has shown that the activation of NF-κBp65 and its downstream targets by fluorosis may disrupt dental embryogenesis and promote the progression of dental fluorosis [35,36]. Our results suggested that NaF significantly increased the expression of Bax, NF-κBp65, and TMEM16A in ameloblasts while decreasing the expression of Bcl-2 and BMP-2. Low, medium, and high calcium treatments significantly reduced the expression of Bax, NF-κBp65, and TMEM16A, while increasing the expression of Bcl-2 and BMP-2, with the highest effectiveness observed in the high calcium group. This indicates that high calcium may affect ameloblast apoptosis by regulating apoptosis-related genes and TMEM16A.

TMEM16A/ANO1, a calcium-activated chloride ion channel (CaCC), plays a pivotal role in modulating various physiological characteristics in response to fluctuation in intracellular calcium concentrations [37]. Overexpression of TMEM16A not only promotes cancer cell proliferation, migration, and invasion but also inhibits apoptosis in these cells, thus affecting tumor growth. Additionally, it is also associated with resistance to cancer treatment, recurrence, and poor prognosis [38]. Research indicated that during advanced stages of intestinal inflammation, TMEM16A inhibits inflammation-induced cell apoptosis by activating the ERK/Bcl-2/Bax signaling pathway [39]. Moreover,

TMEM16A's role in oncology is further substantiated by its association with breast tumor progression. Upregulation of TMEM16A levels leads to increased BCL-2 expression, whereas its downregulation induces cell apoptosis [40]. Furthermore, overexpression of TMEM16A enhances the proliferation, migration, and invasion of glioma cells by activating the NF-κBp65 signaling pathway [41]. Despite its significant role in various conditions such as diarrhea, pain, asthma, hypertension, gastritis, and various cancers [42,43], its precise function in tooth development remains unclear. Our findings suggest that, under high calcium (4.0 mmol/L) culture conditions, the inhibition of TMEM16A expression using the inhibitor T16Ainh-A01 significantly promotes ameloblast cell proliferation, reduces intracellular Ca^{2+} concentrations, and suppresses cell apoptosis. Simultaneously, the inhibition of TMEM16A expression substantially reduces the expression levels of Bax and NF-κBp65 in ameloblast, while significantly increasing the expression levels of Bcl-2 and BMP-2. These findings align with previous in vivo studies [44]. These results suggest that during high-calcium culture conditions, the inhibition of TMEM16A may potentially suppress fluoride-induced ameloblast cell apoptosis by regulating the NF-κBp65 signaling pathway and genes associated with apoptosis.

Conclusion

In conclusion, our study demonstrated that under high calcium conditions, the inhibition of TMEM16A expression can alleviate fluoride-induced ameloblast apoptosis induced by modulating the NF-κBp65 signaling pathway and genes associated with apoptosis. These findings offer valuable insights and a theoretical foundation for further investigations into the occurrence and treatment of dental fluorosis. However, it is crucial to acknowledge the limitations of this study. One limitation is that we did not establish a TMEM16A overexpression cell model, which could offer further insights into the impact of TMEM16A on ameloblast proliferation, apoptosis, and the expression of the related genes. Additionally, further *in vitro* and *in vivo* investigation is needed to determine the specific role of TMEM16A in ameloblast apoptosis induced by fluorosis. Subsequent investigations should focus on establishing these models and exploring the potential clinical implications of these findings in dental treatment. By addressing these limitations and conducting more comprehensive studies, we can gain a deeper understanding of the molecular mechanisms underlying ameloblast apoptosis and develop more effective strategies for the prevention and treatment of dental fluorosis.

Availability of Data and Materials

The datasets analyzed during current study are available from the corresponding author upon reasonable request.

Author Contributions

YYY and YHY designed and performed the research. FX and RL were mainly involved in the acquisition of data and article writing. DRZ and HTL interpreted the data. LFW provided help and advice on the immunohistochemical experiments. All authors contributed to editorial changes in the manuscript. All authors read and approved the final manuscript. All authors have participated sufficiently in the work and agreed to be accountable for all aspects of the work.

Ethics Approval and Consent to Participate

This study was conducted with the authorization of Ethics Committee of Huabei Petroleum Administration Bureau General Hospital (Ethical approval No.: 2020-06).

Acknowledgment

Not applicable.

Funding

Study on the correlation between calcium activated chloride ion channels and the mechanism of dental fluorosis, 20210664.

Conflict of Interest

The authors declare no conflict of interest.

References

[1] Barakat A, Alshehri M, Koppolu P, Alhelees A, Swapna LA. Minimal Invasive Technique for the Esthetic Management of Dental Fluorosis. Journal of Pharmacy & Bioallied Sciences. 2022; 14: S1050–S1053.
[2] Xu YC, Niu HM, Guo WH. Research progress of cell polarity in tooth development. Chinese Journal of Practical Stomatology. 2022; 15: 6.
[3] Zhong WK, He LF, Yu RA. Research Progress on Molecular Mechanism of Dental Fluorosis. Journal of Guangzhou Medical College. 2011; 39: 97–101.
[4] Johnston NR, Strobel SA. Principles of fluoride toxicity and the cellular response: a review. Archives of Toxicology. 2020; 94: 1051–1069.
[5] Wei W, Pang S, Sun D. The pathogenesis of endemic fluorosis: Research progress in the last 5 years. Journal of Cellular and Molecular Medicine. 2019; 23: 2333–2342.
[6] Cox DH. Ca(2+)-regulated ion channels. BMB Reports. 2011; 44: 635–646.
[7] Song JL, Zhang L, Jiang YG, Hou TZ, Li XM. Research on doctor-patient communication of clinical interns in Department of Stomatology. Chinese Medical Ethics. 2005; 18: 60–61.
[8] Ouyang W, Li Y, Liu Z. Effect caused by uptake of different levels of calcium to enamel fluorosis in rats. Chinese Journal of Stomatology. 2000; 35: 47–49.
[9] Hou TZ, Liang J, Tao H. Fluoride inhibits BMP-2 expression in ameloblasts of mouse incisors. Journal of Modern Stomatology. 2005; 19: 3.
[10] Hu X, Li H, Yang M, Chen Y, Zeng A, Wu J, *et al*. Effect of Long Non-coding RNA and DNA Methylation on Gene Expression

in Dental Fluorosis. Biological Trace Element Research. 2024; 202: 221–232.

[11] Osta B, Lavocat F, Eljaafari A, Miossec P. Effects of Interleukin-17A on Osteogenic Differentiation of Isolated Human Mesenchymal Stem Cells. Frontiers in Immunology. 2014; 5: 425.

[12] Xu L, Deng C, Zhang Y, Zhao L, Linghu Y, Yu Y. Expression of Autophagy-Related Factors LC3A and Beclin 1 and Apoptosis-Related Factors Bcl-2 and BAX in Osteoblasts Treated With Sodium Fluoride. Frontiers in Physiology. 2021; 12: 603848.

[13] Gao J, Tian X, Yan X, Wang Y, Wei J, Wang X, *et al*. Selenium Exerts Protective Effects Against Fluoride-Induced Apoptosis and Oxidative Stress and Altered the Expression of Bcl-2/Caspase Family. Biological Trace Element Research. 2021; 199: 682–692.

[14] Jeon D, Jo M, Lee Y, Park SH, Phan HTL, Nam JH, *et al*. Inhibition of ANO1 by *Cis*- and *Trans*-Resveratrol and Their Anticancer Activity in Human Prostate Cancer PC-3 Cells. International Journal of Molecular Sciences. 2023; 24: 1186.

[15] Danahay H, Gosling M. TMEM16A: An Alternative Approach to Restoring Airway Anion Secretion in Cystic Fibrosis? International Journal of Molecular Sciences. 2020; 21: 2386.

[16] Wang L, Zhu Y, Wang D. High-Dose Fluoride Induces Apoptosis and Inhibits Ameloblastin Secretion in Primary Rat Ameloblast. Biological Trace Element Research. 2016; 174: 402–409.

[17] Liu B, Wang P, Wang Z, Zhang W. The use of anti-VDAC2 antibody for the combined assessment of human sperm acrosome integrity and ionophore A23187-induced acrosome reaction. PloS One. 2011; 6: e16985.

[18] Li K, Xue Y, Chen A, Jiang Y, Xie H, Shi Q, *et al*. Heat shock protein 90 has roles in intracellular calcium homeostasis, protein tyrosine phosphorylation regulation, and progesterone-responsive sperm function in human sperm. PloS One. 2014; 9: e115841.

[19] Gupta SK, Khan TI, Gupta RC, Gupta AB, Gupta KC, Jain P, *et al*. Compensatory hyperparathyroidism following high fluoride ingestion - a clinico - biochemical correlation. Indian Pediatrics. 2001; 38: 139–146.

[20] Kebede A, Retta N, Abuye C, Whiting SJ, Kassaw M, Zeru T, *et al*. Dietary Fluoride Intake and Associated Skeletal and Dental Fluorosis in School Age Children in Rural Ethiopian Rift Valley. International Journal of Environmental Research and Public Health. 2016; 13: 756.

[21] Yu J, Jun D, Wang W, Xu C, Wu Y, Shi Y, *et al*. Changes of serum parathyroid hormone in rats with fluorosis under different calcium nutrition conditions. Chinese Journal of Endemic Diseases. 2006; 25: 4.

[22] Mehta DN, Shah J. Reversal of dental fluorosis: A clinical study. Journal of Natural Science, Biology, and Medicine. 2013; 4: 138–144.

[23] An X, Fu R, Ma P, Ma X, Fan D. Ginsenoside Rk1 inhibits cell proliferation and promotes apoptosis in lung squamous cell carcinoma by calcium signaling pathway. RSC Advances. 2019; 9: 25107–25118.

[24] Barry EL. Expression of mRNAs for the alpha 1 subunit of voltage-gated calcium channels in human osteoblast-like cell lines and in normal human osteoblasts. Calcified Tissue International. 2000; 66: 145–150.

[25] Bernard-Marissal N, Moumen A, Sunyach C, Pellegrino C, Dudley K, Henderson CE, *et al*. Reduced calreticulin levels link endoplasmic reticulum stress and Fas-triggered cell death in motoneurons vulnerable to ALS. The Journal of Neuroscience: the Official Journal of the Society for Neuroscience. 2012; 32: 4901–4912.

[26] Zhang Y, Ma L, Li J, Zhong M, Zhang KQ, Gu HF. Experimental study on calcium overload and apoptosis induced by excessive fluoride in ameloblasts. West China Journal of Stomatology. 2014; 32: 5. (in Chinese)

[27] Wang H, Hu X, Li M, Pan Z, Li D, Zheng Q. Daphnoretin induces reactive oxygen species-mediated apoptosis in melanoma cells. Oncology Letters. 2021; 21: 453.

[28] Liu YL, Yang WH, Chen BY, Nie J, Su ZR, Zheng JN, *et al*. miR 29b suppresses proliferation and induces apoptosis of hepatocellular carcinoma ascites H22 cells via regulating TGF β1 and p53 signaling pathway. International Journal of Molecular Medicine. 2021; 48: 157.

[29] Han L, Han B. Effects of fluoride on the gene expression of Bcl-2 and Bax in sheep osteoblasts cultured *in vitro*. Chinese Journal Veterinary. 2010; 46: 3–6.

[30] Zhao YD, Hou TZ, Gou JC, Wang DY, Yao HB, Liang J, *et al*. Experimental study on the effect of fluoride on the expression of Bcl-2 and Bax in mouse ameloblasts. Shanxi Medical Journal. 2004; 33: 3.

[31] Jiang N, Chen L, Ma Q, Ruan J. Nanostructured Ti surfaces and retinoic acid/dexamethasone present a spatial framework for the maturation and amelogenesis of LS-8 cells. International Journal of Nanomedicine. 2018; 13: 3949–3964.

[32] Liu M, Goldman G, MacDougall M, Chen S. BMP Signaling Pathway in Dentin Development and Diseases. Cells. 2022; 11: 2216.

[33] Ji ZZ, Xia R, Mei LX. The effect of short-term high concentration fluoride on the expression of BMP-2 in mouse molar ameloblasts. Chinese Medical Science. 2012; 2: 3.

[34] Zhang KL, Yuan CX, Guan ZZ. Expression levels of P-glycoprotein and nuclear factor-κB in liver of rats with chronic fluorosis. Journal of Guiyang Medical College. 2014; 817–819.

[35] Castaneda B, Simon Y, Jacques J, Hess E, Choi YW, Blin-Wakkach C, *et al*. Bone resorption control of tooth eruption and root morphogenesis: Involvement of the receptor activator of NF-κB (RANK). Journal of Cellular Physiology. 2011; 226: 74–85.

[36] Chen L, Kuang P, Liu H, Wei Q, Cui H, Fang J, *et al*. Sodium Fluoride (NaF) Induces Inflammatory Responses Via Activating MAPKs/NF-κB Signaling Pathway and Reducing Anti-inflammatory Cytokine Expression in the Mouse Liver. Biological Trace Element Research. 2019; 189: 157–171.

[37] Peters CJ, Yu H, Tien J, Jan YN, Li M, Jan LY. Four basic residues critical for the ion selectivity and pore blocker sensitivity of TMEM16A calcium-activated chloride channels. Proceedings of the National Academy of Sciences of the United States of America. 2015; 112: 3547–3552.

[38] Luo S, Wang H, Bai L, Chen Y, Chen S, Gao K, *et al*. Activation of TMEM16A Ca^{2+}-activated Cl^- channels by ROCK1/moesin promotes breast cancer metastasis. Journal of Advanced Research. 2021; 33: 253–264.

[39] Bai W, Liu M, Xiao Q. The diverse roles of TMEM16A Ca^{2+}-activated Cl^- channels in inflammation. Journal of Advanced Research. 2021; 33: 53–68.

[40] Mezzatesta C, Abduli L, Guinot A, Eckert C, Schewe D, Zaliova M, *et al*. Repurposing anthelmintic agents to eradicate resistant leukemia. Blood Cancer Journal. 2020; 10: 72.

[41] Takayasu T, Kurisu K, Esquenazi Y, Ballester LY. Ion Channels and Their Role in the Pathophysiology of Gliomas. Molecular Cancer Therapeutics. 2020; 19: 1959–1969.

[42] Ji Q, Guo S, Wang X, Pang C, Zhan Y, Chen Y, *et al*. Recent advances in TMEM16A: Structure, function, and disease. Journal of Cellular Physiology. 2019; 234: 7856–7873.

[43] Seo Y, Lee HK, Park J, Jeon DK, Jo S, Jo M, *et al*. Ani9, A Novel Potent Small-Molecule ANO1 Inhibitor with Negligible Effect on ANO2. PloS One. 2016; 11: e0155771.

[44] Yangyang Y, Rong L, Fei X, Yahui Y. Unraveling the Mechanisms of TMEM16A in Fluoride Toxicity and Tooth Development. Journal of Biological Regulators and Homeostatic Agents. 2023; 37: 6015–6027.